PAPER *Special Section on Intelligent Transport Systems and Wideband Systems*

Performance Evaluation of Wi-Fi RTT Lateration without Pre-Constructing a Database

Tetsuya MANABE[†a)], ***Senior Member and*** **Kazuya SABA**[††], ***Nonmember***

SUMMARY This paper proposes an algorithm for estimating the location of wireless access points (APs) in indoor environments to realize smartphone positioning based on Wi-Fi without pre-constructing a database. The proposed method is designed to overcome the main problem of existing positioning methods requiring the advance construction of a database with coordinates or precise AP location measurements. The proposed algorithm constructs a local coordinate system with the first four APs that are activated in turn, and estimates the AP installation location using Wi-Fi round-trip time (RTT) lateration and the ranging results between the APs. The effectiveness of the proposed algorithm is confirmed by conducting experiments in a real indoor environment consisting of two rooms of different sizes to evaluate the positioning performance of the algorithm. The experimental results showed the proposed algorithm using Wi-Fi RTT lateration delivers high smartphone positioning performance without a pre-constructed database or precise AP location measurements.

key words: *Wi-Fi RTT, WLAN RTT, round-trip time, ranging, lateration, local coordinate system, location configuration information report, LCI report*

1. Introduction

The demand for location-based services (LBSs), which require the geographical location of a mobile phone, is growing with the popularization of smartphones. The provision of high-quality LBSs requires highly accurate and precise location information, because the quality of LBSs depends on the positioning performance. Global navigation satellite system (GNSS) is widely used as a positioning technology, but it is known to cause large errors or results are not obtained in non-open-sky environments, e.g., urban canyons, underground, and indoors. By the way, Japanese people reportedly spend 90% of their daily time on weekdays and 88% thereof on holidays indoors (e.g. [1]); thus, accurate and precise positioning is important, particularly indoors. There are some positioning techniques based on radio waves, such as Wi-Fi and ultra-wideband (UWB), which can be used in indoor environments. UWB uses short time-length pulses to measure distance and shape. It can be used in some smartphone models. However, UWB requires the installation of dedicated tags for positioning. On the other hand, Wi-Fi is equipped as a standard feature in many smartphones. Wi-Fi access points (APs) are already installed for communication in various places, such as private homes, offices, stores, and public facilities. These APs can also be used for smartphone positioning. Thus, Wi-Fi is widely used to determine the positions of smartphones in indoor environments. Typical positioning algorithms for Wi-Fi include proximity [2], fingerprint [3], [4], and lateration [5] algorithms. The proximity algorithm regards the device location as the position of the closest AP at which the strongest received signal strength (RSS) has been observed. This algorithm is commonly used for rough positionings such as check-in and area identification. The fingerprint algorithm identifies the device location probabilistically from a database (DB) consisting of reference information of locations, the unique identifier (e.g., the media access control address and basic service set identifier) of the AP, and RSS. This algorithm is the most widely used on smartphones. To realize highly accurate and precise positioning using the fingerprint algorithm, the DBs need to include sufficient training data, the acquisition of which is time-consuming and requires considerable effort (e.g. [6]). The lateration algorithm entails the calculation of the distance between the AP and the mobile device. If the location (x_p, y_p, z_p) of the mobile device is unknown, it can be identified by solving a three-way simultaneous quadratic equation from the coordinates of three known APs. Although RSS is widely used for ranging (distance measurement) on Wi-Fi, its performance is greatly affected by radio-wave fluctuations, and its positioning performance has been reported to be inferior to that of the fingerprint algorithm [7]. Time-based ranging over Wi-Fi has also been proposed [8], and efforts have been made to improve its performance (e.g., [9], [10]). However, this method requires specialized equipment and is not compatible with smartphones. On the other hand, the method of the Wi-Fi (WLAN) round-trip time (RTT) was standardized in 2016 as IEEE 802.11-2016 [11]. This method measures the RTT of packets between a responder (e.g., an access point) and an initiator (e.g., a smartphone) and is a standard component of Android 9 (Pie). In other words, commercially available smartphones and APs can now be used for time-based ranging and positioning. As a result, many research groups are currently focusing on Wi-Fi RTT in their studies [12]–[35]. These existing research efforts on Wi-Fi RTT-based positioning methods assume that the location of the APs is known, that is, that administrators set the AP location information in advance.

Incidentally, the fine timing measurement (FTM) used in Wi-Fi RTT includes the location configuration informa-

Manuscript received May 5, 2022.
Manuscript revised September 10, 2022.
Manuscript publicized December 2, 2022.

[†]The author is with the Graduate School of Science and Engineering, Saitama University, Saitama-shi, 338-8570 Japan.
[††]The author was with the Faculty of Engineering, Saitama University, Saitama-shi, 338-8570 Japan.
a) E-mail: manabe@mnb.ees.saitama-u.ac.jp

DOI: 10.1587/transfun.2022WBP0001

tion report (LCI report), which is used to send the location of the responder (e.g., an access point) to the initiator (e.g., a smartphone) [11]. In addition, ranging by Wi-Fi RTT can be performed not only between smartphones and APs, but also between APs. In other words, APs that support Wi-Fi RTT can estimate their own installation location by ranging each other. The estimated location of the APs can then be sent to smartphones via LCI reports. These mechanisms eliminate the pre-construction of a DB, which was essential for conventional Wi-Fi-based positioning. Against this background, the algorithm we propose for estimating the location of APs realizes Wi-Fi RTT lateration without the need to pre-construct a DB and without requiring precise measurement of the AP installation location. The performance of the method is then evaluated by carrying out experiments in real indoor environments.

2. Wi-Fi RTT Ranging, Positioning, and LCI Report

2.1 Wi-Fi RTT Ranging

Figure 1 illustrates the basic principle of Wi-Fi RTT. A station (STA; initiator) transmits an FTM request to an access point (AP; responder). The AP transmits an FTM message to the STA, and the STA receiving the FTM message performs an acknowledgment (ACK) transmission. At this time, the AP records the time at which the FTM message is transmitted, t_1, and the time at which the ACK is received, t_4, and the STA records the FTM message reception time, t_2, and the ACK transmission time, t_3. The AP then places t_1 and t_4 into an FTM message and transmits it to the STA. As a result, because t_1, t_2, t_3, and t_4 are aligned in the STA, the RTT is calculated. To improve the measurement accuracy, RTT is determined by calculating the average of m round trips as expressed by Eq. (1).

$$RTT = \frac{1}{m}\left(\sum_{k=1}^{m}(t_4(k)-t_1(k))-\sum_{k=1}^{m}(t_3(k)-t_2(k))\right) \quad (1)$$

Then, the AP-STA distance, d, is calculated using $d = RTT \cdot c/2$, where, c is the speed of electromagnetic wave propagation. The STA and AP clocks do not need to be synchronized as the time differences between readings taken by the same clock are calculated. The ranging performance of Wi-Fi RTT in real environments has been evaluated [12], [13].

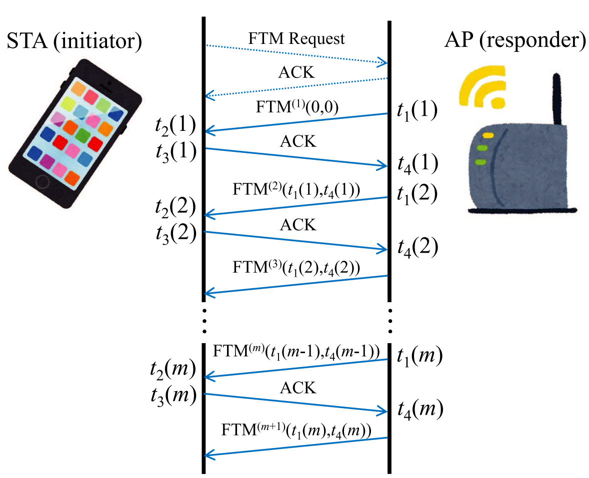

Fig. 1 Wi-Fi RTT basic principle.

2.2 Positioning Based on Wi-Fi RTT Ranging

Wi-Fi RTT ranging can determine the distance between an initiator and a responder (e.g., between a smartphone and an AP, or between two APs), thus the lateration algorithm is generally used as the positioning method. As described in Sect. 1, if the location (x_p, y_p, z_p) of an initiator is unknown, it can be identified by solving a three-way simultaneous quadratic equation from the coordinates of three known responders. The simultaneous equation for lateration is as follows:

$$d_i = \sqrt{(x_i - x_p)^2 + (y_i - y_p)^2 + (z_i - z_p)^2}, \quad (2)$$

where, $i = 1, 2, \cdots, n$ (n is the number of responders), (x_p, y_p, z_p) is the initiator's position, (x_i, y_i, z_i) is the i-th responder's position, and d_i is the distance between the initiator and the i-th responder. The value of d_i is determined using the Wi-Fi RTT ranging method described in Sect. 2.1. The simultaneous equation is generally solved using least-squares methods, which employ the following calculation procedure:

Step-1 Set an appropriate initial value (x_0, y_0, z_0) to the initiator coordinate (x_p, y_p, z_p), which is an unknown number.

Step-2 Obtain ΔR_i using the value of d_i and the initial initiator coordinate values (x_0, y_0, z_0) set in **Step-1**.

$$\Delta R_i = d_i - \rho_i, \quad (3)$$

where,

$$\rho_i = \sqrt{(x_i - x_0)^2 + (y_i - y_0)^2 + (z_i - z_0)^2}. \quad (4)$$

Step-3 The unknown matrix $\mathbf{A}$ given by

$$\mathbf{A} = \begin{pmatrix} -(x_1 - x_0)/\rho_1 & -(y_1 - y_0)/\rho_1 & -(z_1 - z_0)/\rho_1 \\ -(x_2 - x_0)/\rho_2 & -(y_2 - y_0)/\rho_2 & -(z_2 - z_0)/\rho_2 \\ & \vdots & \\ -(x_n - x_0)/\rho_n & -(y_n - y_0)/\rho_n & -(z_n - z_0)/\rho_n \end{pmatrix} \quad (5)$$

is calculated from the matrix $\Delta\mathbf{R} = (\Delta R_1, \Delta R_2, \cdots, \Delta R_n)^{\mathsf{T}}$ obtained from Eq. (3) and the matrix $\Delta\mathbf{X} = (\Delta x, \Delta y, \Delta z)^{\mathsf{T}}$ of the initiator coordinate modification values, where,

$$\Delta\mathbf{R} = \mathbf{A}\Delta\mathbf{X} + \boldsymbol{\varepsilon}, \quad (6)$$

and $\boldsymbol{\varepsilon} = (\varepsilon_1, \varepsilon_2, \cdots, \varepsilon_n)^{\mathsf{T}}$ is the error component.

Step-4 Find $\Delta\mathbf{X}$ given by

$$\Delta\mathbf{X} = (\mathbf{A}^{\mathsf{T}}\mathbf{A})^{-1}\mathbf{A}^{\mathsf{T}}\Delta\mathbf{R}, \tag{7}$$

where the calculation is performed such that the error $\boldsymbol{\varepsilon}$ in Eq. (6) is minimized.

Step-5 Determine whether the elements $(\Delta x, \Delta y, \Delta z)$ of $\Delta\mathbf{X}$ calculated by Eq. (7) are sufficiently small. If sufficiently small, output (x_0, y_0, z_0) as the solution. If not, add $(\Delta x, \Delta y, \Delta z)$ to (x_0, y_0, z_0) and return to **Step-2**.

Various researchers [14]–[16] have evaluated the positioning performance using Wi-Fi RTT ranging in real environments. Unuma et al. [17] showed that positioning performance based on Wi-Fi RTT ranging equal to or superior to that of the conventional fingerprint algorithm can be obtained with a reduced number of APs. Si et al. [18] proposed a positioning method with line-of-sight/non-line-of-sight identification to enhance the positioning accuracy. Yu et al. [19] proposed a calibration, filtering, and modeling algorithm that can effectively reduce the ranging error caused by clock deviation, non-line-of-sight, and multipath propagation. Ma et al. [20] proposed a systematic bias removal process for improving the ranging accuracy, and proposed a positioning method based on clustering-based lateration with the generation of weighted concentric circles. Other research aimed to improve the positioning performance by using machine learning [21]–[24] or by combining Wi-Fi RTT-based positioning methods with other methods such as map information [25], [26], RSS-based ranging [27], sensors [28]–[32], radio detection and ranging (RADAR) [33], and radio fusion (ultra-wideband and cellular) [34]. These previous research studies on Wi-Fi RTT-based positioning methods assume that the locations of the APs are known in advance. In other words, it is necessary to precisely measure the AP installation locations in advance and to either construct a database of these locations or register the information within each AP. On the other hand, Choi et al. [35] developed an unsupervised learning technique to obtain the coordinates of unknown APs that coexist with anchor APs. Although it is possible to reduce the number of AP locations that need to be pre-registered, the locations of anchor APs must be measured precisely in advance, as in previous research [14]–[34]. In this study, a local coordinate system is used to realize Wi-Fi RTT lateration without prior measurement of the locations of APs.

2.3 FTM-Related Field Format

Figure 2 shows the field format related to the FTM used in Wi-Fi RTT. The location configuration information (LCI) field is formatted as shown in Fig. 2(a). This structure and the information fields are based on the LCI format described in the Request for Comments (RFC) 6225[†] by the Internet Engineering Task Force (IETF). The interpretation of the altitude value depends on the value of the Altitude Type

[†]https://datatracker.ietf.org/doc/html/rfc6225

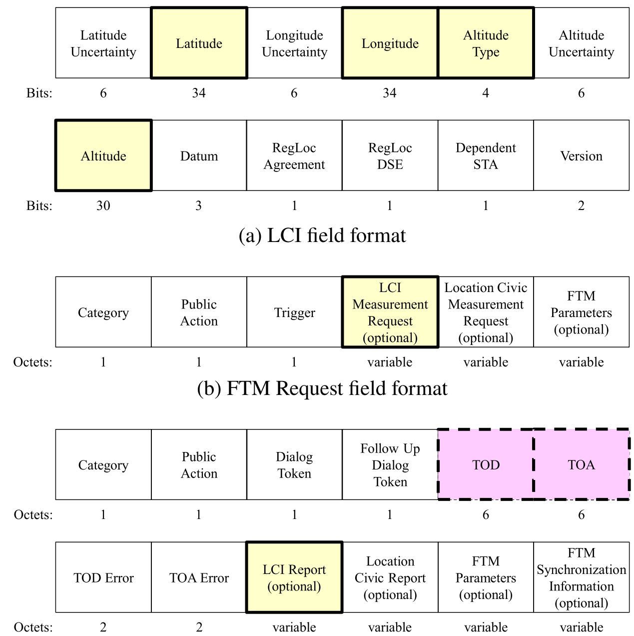

(a) LCI field format

(b) FTM Request field format

(c) FTM field format

Fig. 2 FTM-related field format.

(AType). If AType = 1, the altitude is measured in meters, in relation to the zero set by the vertical datum. The format of the FTM Request field is shown in Fig. 2(b). This field contains an LCI Measurement Request field; however, the inclusion of this field is optional. If present, the field indicates a request for a Measurement Report element. The format of the FTM field is shown in Fig. 2(c). The time of departure (TOD) and the time of arrival (TOA) fields for calculating the round-trip time are expressed in units of picoseconds, that is, the theoretical ranging resolution is 0.3 mm. However, the realistic measurement accuracy is in the nanosecond to sub-nanosecond range (e.g., [36]), that is, the ranging resolution is 30 to 3 cm range. The inclusion of the LCI Report field is optional. If present, the field contains the LCI Report field formatted as shown in Fig. 2(a). Thus, the LCI report can be used to send the AP installation location to smartphones. The advantage of this report is that it eliminates the need to pre-construct DBs with the required positioning information, which was essential for conventional Wi-Fi-based positioning. The algorithm proposed in this paper for estimating the AP installation locations uses a local coordinate system to send these locations in the form of the LCI report. The proposed algorithm uses the locations in the LCI report in conjunction with Wi-Fi RTT lateration for positioning. In addition, we evaluate its performance by conducting ranging and positioning experiments in real indoor environments using Wi-Fi RTT lateration.

3. Algorithm for Estimating the AP Installation Location

In this section, we propose the algorithm for estimating the AP installation locations using Wi-Fi RTT to realize the positioning system. This approach obviates the need to preconstruct a database and to precisely measure the AP locations in advance. The proposed algorithm is based on the following precondition and assumption.

- Wi-Fi APs are usually installed in the same location for an extended period of time.
- To determine the smartphone position using the lateration algorithm, four or more APs are installed in the environment (henceforth, the number of APs installed is denoted by n).
- All the APs are based on IEEE 802.11-2016 [11] and include the ability to send an FTM message and LCI report.
- All the APs can measure the distance between each other by Wi-Fi RTT. This functionality is included in IEEE 802.11-2016 [11].
- Wi-Fi RTT ranging results include a certain degree of bias error, but are extremely stable (e.g., [13]), and the bias error can be removed systematically (e.g., [20]).
- The rough location of all APs is known because the APs must be activated in sequence.
- APs are activated one at a time, in the specified order.
- The local coordinate system used for APs uses $x-$, $y-$, z-coordinates, and all the APs are set at $x \geq 0$, $y \geq 0$, and $z \geq 0$.
- The coordinate system in real space, e.g., the space in which people move, uses $X-, Y-, Z$-coordinates.

Figure 3 shows the basic principle of the proposed algorithm, which has the following operating procedure:

Step-1 Activate the first AP as AP_1, and set AP_1 as the origin of the local coordinate system (i.e., $\mathrm{AP}_1(0,0,0)$).

Step-2 Activate the second AP as AP_2, and measure the distance ($d_{2,1}$) from AP_2 to AP_1 by Wi-Fi RTT ranging. The x-axis of the local coordinate system is set to pass through AP_1 and AP_2, and the x-coordinate (x_2) of AP_2 is set to $d_{2,1}$. Note that the y- and z-coordinates of AP_2 are set to zero. Thus, $\mathrm{AP}_2(x_2, 0, 0)$ is obtained. Here, $x_2 = d_{2,1}$.

Step-3 Activate the third AP as AP_3, and measure the distances ($d_{3,1}$ and $d_{3,2}$) from AP_3 to AP_1 and AP_2 by Wi-Fi RTT ranging, respectively. The coordinates of AP_3 are calculated by the lateration algorithm, that described in Sect. 2.2, using the AP coordinates ($\mathrm{AP}_1(0,0,0)$ and $\mathrm{AP}_2(x_2,0,0)$) and the measured distances ($d_{3,1}$ and $d_{3,2}$). Here, the y-axis of the local coordinate system is set as the three activated APs ($\mathrm{AP}_1 \sim \mathrm{AP}_3$) form a plane S_{123}. Thus, the coordinates of $\mathrm{AP}_3(x_3, y_3, 0)$ are obtained. Here, $x_3 \geq 0$ and $y_3 > 0$.

Step-4 In this algorithm, all the APs are set at $x \geq 0$, $y \geq 0$, and $z \geq 0$. Therefore, the coordinate system (right-handed or left-handed) is determined by the order in which the APs are activated. In other words, the positive direction of the z-axis is determined by the fourth AP. Then, activate the fourth AP as AP_4, and measure the distances ($d_{4,1}$, $d_{4,2}$, and $d_{4,3}$) from AP_4 to the other activated APs by Wi-Fi RTT ranging, respectively. The coordinates of AP_4 are calculated by the lateration algorithm. Here, the z-axis of the local coordinate system is set perpendicular to the plane S_{123} and such that it passes through the origin. Thus, the coordinates of $\mathrm{AP}_4(x_4, y_4, z_4)$ are obtained. Here, $x_4 \geq 0$, $y_4 \geq 0$, and $z_4 > 0$.

Step-5 If five or more APs exist, activate the next AP as AP_k ($5 \leq k \leq n$), and calculate the coordinates of AP_k using the lateration algorithm described in Sect. 2.2, the AP coordinates ($\mathrm{AP}_1(0,0,0) \sim \mathrm{AP}_{k-1}(x_{k-1}, y_{k-1}, z_{k-1})$, where $y_2 = z_2 = z_3 = 0$), and the measured distances ($d_{k,1} \sim d_{k,k-1}$). Repeat this procedure for the remaining number of APs.

This algorithm constructs a local coordinate system with the first four APs ($\mathrm{AP}_1 \sim \mathrm{AP}_4$) that are activated in turn. Therefore, the coordinate systems in real space (i.e., X, Y, Z axes) and the local coordinate system of the AP (i.e., x, y, z axes) may not correspond to each other as shown in Fig. 4(a). The two coordinate systems do not have to coincide to be used in positioning systems. However, should it be more intuitive to use the same coordinate systems (especially the same horizontal plane), e.g., in navigation systems, the $XY-$ and $xy-$planes can be easily set to be parallel by requiring the height of the first three APs to be activated to be the same, as in Fig. 4(b). In this case, only the heights of the AP need to be the same, e.g., setting on a ceiling, and the specific values are arbitrary. Thus, a positioning system can

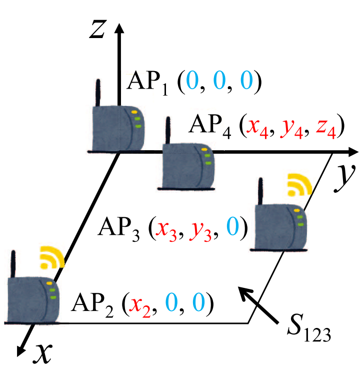

Fig. 3 Coordinates of the APs used by the algorithm for estimating the AP installation locations.

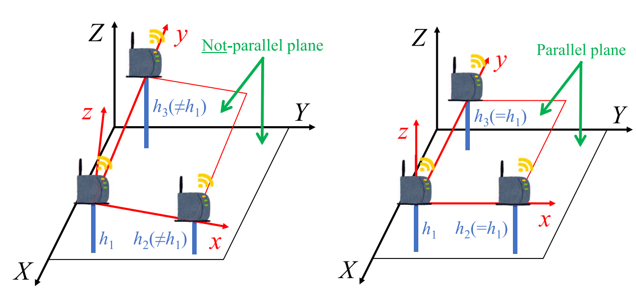

(a) First three APs installed at different heights

(b) First three APs installed at the same heights

Fig. 4 AP installation heights and coordinate planes used by the algorithm for estimating the AP installation locations.

be realized without prior database construction or precise measurements of AP installation locations.

4. Experiment for Performance Evaluation

4.1 Overview

Experiments were conducted to evaluate the positioning performance of the proposed algorithm in real indoor environments to confirm its effectiveness. In these experiments, the performance in terms of estimating the AP installation location and position of the smartphone was evaluated by specifying fixed horizontal coordinates for the AP installation location. These coordinates were used to evaluate the influence of the height at which the APs were installed and the order in which the APs were activated (which affects the settings of the coordinate system) on the positioning performance of the algorithm. The experimental environment consists of two rooms of different sizes, as shown in Fig. 5. The first room is a small seminar room (7.2×5.5 m with a seating capacity of approximately 30 persons), and the second room is a large lecture room (14.7×9.3 m with a seating capacity of 154 persons). We used the Google Pixel 3 smartphone as the testbed and the Compulab fitlet2 FTM Responder device† as the AP in this experiment. The smartphone was mounted on a tripod at a fixed height of 1.2 m above the floor to simulate use by a standing human. The APs were set to the 5-GHz band at 40-MHz bandwidth (38 or 46 ch). These settings previously delivered the best positioning performance [12] and ensured that the channels in the experimental environments were less crowded. In this evaluation experiment, we used six APs that were placed according to the following criteria. One AP was placed at each of the four corners of the room, i.e., at P_a, P_b, P_c, and P_d in Fig. 5. The other two APs were placed at the center of gravity of $\triangle P_aP_bP_c$ and $\triangle P_bP_cP_d$, respectively, i.e., P_e and P_f in Fig. 5. The patterns that were used to evaluate the height at which the AP was installed and the order in which APs were activated are listed in Table 1. Two AP installation heights were used: high (2.495 m; [H]) and low (2.000 m; [L]). Our previous research [37] showed that the ranging performance was worse for APs installed at lower heights. Thus, we evaluate different combinations of AP installation heights to confirm that the proposed method is effective regardless of the AP installation height. "HH" means that all APs were installed at the higher position. "HL" means that one AP was installed at the lower position and all others were installed at the higher position. "L" means that four APs, which affect the coordinate system settings, were installed at the lower position and all others were installed at the higher position. The order in which the APs were activated was varied by using four different sequences that delivered relatively high performance in the numerical simulation prior to the experiment. These APs were under the line-of-sight (LoS) condition with each other in all experimental patterns. The bias error in ranging

†https://fit-iot.com/web/products/wild/

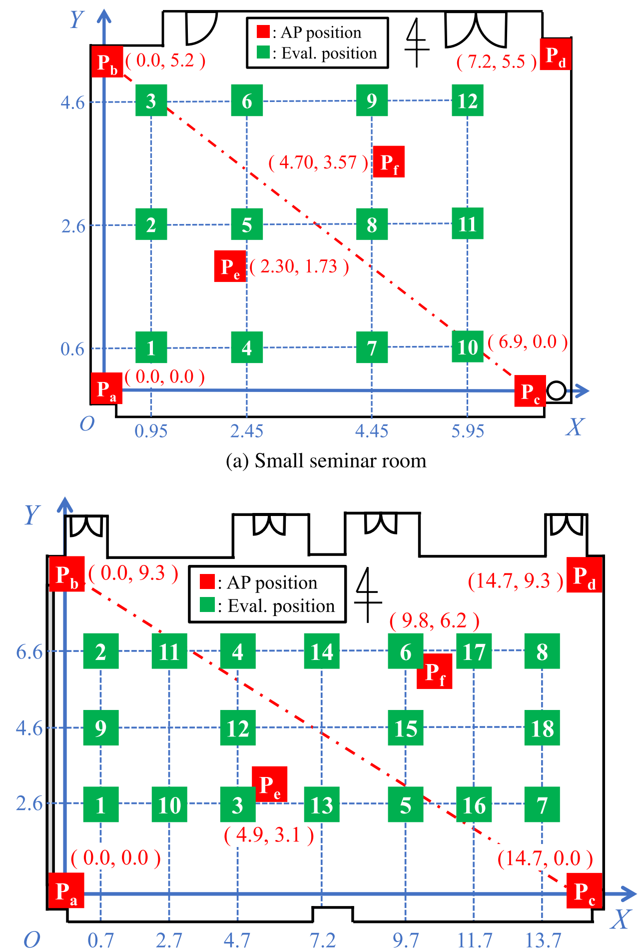

(a) Small seminar room

(b) Large lecture room

Fig. 5 Experimental environment (unit: meter).

Table 1 Evaluation patterns.

	AP_1	AP_2	AP_3	AP_4	AP_5	AP_6
HH_abe	P_a[H]	P_b[H]	P_e[H]	P_c[H]	P_d[H]	P_f[H]
HH_abf	P_a[H]	P_b[H]	P_f[H]	P_d[H]	P_e[H]	P_c[H]
HH_ace	P_a[H]	P_c[H]	P_e[H]	P_b[H]	P_d[H]	P_f[H]
HH_acf	P_a[H]	P_c[H]	P_f[H]	P_d[H]	P_e[H]	P_b[H]
HL_abe	P_a[H]	P_b[H]	P_e[H]	P_c[H]	P_d[L]	P_f[H]
HL_abf	P_a[H]	P_b[H]	P_f[H]	P_d[L]	P_e[H]	P_c[H]
HL_ace	P_a[H]	P_c[H]	P_e[H]	P_b[H]	P_d[L]	P_f[H]
HL_acf	P_a[H]	P_c[H]	P_f[H]	P_d[L]	P_e[H]	P_b[H]
L_abc	P_a[L]	P_b[L]	P_c[L]	P_d[L]	P_e[H]	P_f[H]
L_abd	P_a[L]	P_b[L]	P_d[L]	P_c[L]	P_e[H]	P_f[H]
L_acb	P_a[L]	P_c[L]	P_b[L]	P_d[L]	P_e[H]	P_f[H]
L_acd	P_a[L]	P_c[L]	P_d[L]	P_b[L]	P_e[H]	P_f[H]

"[]" signifies the AP installation height, i.e., [H] is 2.495 m and [L] is 2.000 m.

between APs and between APs and smartphones was 0.22 m (mean value under the LoS environment) and 0.38 m (mean value under both of the LoS and non-LoS (NLoS) environments), respectively, in our prior ranging experiments using the same devices. Therefore, in the experiment in this paper, the bias error in ranging was removed by setting the results of ranging between APs to −0.22 m and between APs and

Table 2 Number of evaluations in each experimental environment.

	Number of evaluating directions 4	2	N_e
Small seminar room	#1~#12	—	48
Large lecture room	#1~#8	#9~#18	52

smartphones to −0.38 m.

To estimate the location at which APs were installed, Wi-Fi RTT was used to measure the distances between APs 1200 times† for each pair. The position of the smartphone was estimated by performing Wi-Fi RTT ranging at each evaluation position in Fig. 5. At each of these positions, the experimenter took 65 measurements in each of four or two directions. Because the large lecture room contains fixed tables, the measurements were taken in two directions in line with the aisles. The reason for measuring in four or two directions was to include the presence or absence of radio wave shielding by the smartphone user (i.e., the measurer in the experiment). The measurer stood in front of the smartphone and in a place where he/she could operate the screen. In other words, the radio waves from the AP in the direction behind the measurer were measured under NLoS, and those from the other APs were measured under LoS conditions. Table 2 provides the number of evaluations in each experimental environment.

The evaluation indexes of the estimation of the AP installation location are the mean error $\overline{e}$, the standard deviation (S.D.) of error σ, and the mean distance error $\overline{e_d}$. Let p_{ij} denote the i-th estimated result of the j-th AP installation location. The mean value of the estimated locations of the j-th AP ($\overline{p_j}$) is expressed by the following equation.

$$\overline{p_j} = \frac{1}{N_m}\sum_{i=1}^{N_m} p_{ij}, \tag{8}$$

where N_m is the number of measurements for each AP (N_m = 1200 in this study). Then, the evaluation indexes ($\overline{e}$, σ, and $\overline{e_d}$) for the entire evaluation area with the number of evaluations (including evaluation points and directions) N_e are obtained from the following equations.

$$\overline{e} = \frac{1}{N_e}\sum_{j=1}^{N_e}(\overline{p_j} - P_j), \tag{9}$$

$$\sigma = \sqrt{\frac{1}{N_e N_m}\sum_{j=1}^{N_e}\sum_{i=1}^{N_m}(p_{ij} - \overline{p_j})^2}, \tag{10}$$

$$\overline{e_d} = \frac{1}{N_e N_m}\sum_{j=1}^{N_e}\sum_{i=1}^{N_m}|p_{ij} - P_j|, \tag{11}$$

where P_j are the true-value coordinates of the j-th AP and the values of N_e are provided in Table 2.

The indexes used to evaluate the estimation of the smartphone position are the horizontal distance error e_{hd} and the positioning result acquisition rate. The horizontal distance error e_{hd} is calculated by

$$e_{hd} = \sqrt{(x_p - x_t)^2 + (y_p - y_t)^2}, \tag{12}$$

where (x_p, y_p) is the estimated smartphone position and (x_t, y_t) is the true position. In this experiment, we obtained the true position (x_t, y_t) using a tape measure set on the floor in the rooms. The acquisition rate of the positioning result is the number of times the positioning result was calculated, i.e., the convergence of Eq. (7) to the solution, out of the total number of measurements. The total number of measurements was 3,120†† in the small seminar room and 3,380††† in the large lecture room.

4.2 Results of AP Installation Location Estimation

Table 3 presents the results of the estimation of the AP installation location. Focusing on the mean distance error, the $x-$ and $y-$coordinates improved by approximately 1 m, whereas the $z-$coordinate declined slightly by approximately 2~3 m for most evaluation patterns. In addition, for "HH(HL)_abe" both the mean error and mean distance error of the z-coordinate were larger than those of the other experiments. On the other hand, there was no significant difference in AP installation location estimation performance by AP installation height. The reasons are discussed in the next section on the basis of the results obtained for the estimation of the smartphone position.

4.3 Results of Smartphone Position Estimation

Figure 6 shows the cumulative probability of horizontal distance errors and Table 4 lists the mean errors in the horizontal distance and the acquisition rate of the positioning result. For the purpose of comparison, the results based on the true value of the AP installation location obtained in the previous study are included in the figure and table and denoted as "Manual."

As shown in Fig. 6(a), (b), (d), and (e), the performance of "HH(HL)_abe" was generally low. The tendency is the same as in Table 3. As shown in Fig. 6(d), (e), and (f), the performance in the large lecture room was lower than that in the small seminar room, but the performance in the large lecture room was similar or very close to that of "Manual," except for "HH(HL)_abe." The worst performing evaluation pattern, "HH(HL)_abe," uses APs located at two positions (P_b and P_e) close to P_a for constructing the coordinate system, whereas the other patterns use APs located far from P_a, i.e., P_c and P_f. As shown in Fig. 6(a), (b), and (c), the performance in the small seminar room was clearly higher

†Measurements were conducted for 20 min in increments of 1 s. The reasons for the 20-minute duration are as follows. Wi-Fi APs usually remain installed in the same location for a long time. Furthermore, our prior experiments confirmed that the cumulative error of Wi-Fi RTT ranging in a LoS environment converges in approximately 1000 seconds.

††65 measurements per time and 48 evaluations.

†††65 measurements per time and 52 evaluations.

Table 3 Results of the estimation of the AP installation location.

Experimental environment	Evaluation pattern	$\overline{e}$ (Mean error) [m]			σ (S.D. of error) [m]			$\overline{e_d}$ (Mean distance error) [m]			
		x	y	z	x	y	z	x	y	z	$\sqrt{x^2+y^2+z^2}$
Small seminar room	HH_abe	2.05	−2.93	5.44	1.16	3.62	1.82	2.05	3.64	5.44	6.86
	HH_abf	2.07	−0.74	3.61	1.11	1.21	1.16	2.07	1.21	3.61	4.33
	HH_ace	1.12	−1.48	5.04	1.07	3.51	1.69	1.16	3.24	5.04	6.10
	HH_acf	1.11	1.34	−1.22	1.01	0.64	2.64	1.14	1.34	3.20	3.65
	HL_abe	2.08	−0.92	4.21	1.12	1.82	1.52	2.08	1.64	4.21	4.97
	HL_abf	2.04	−0.67	3.89	1.03	1.50	1.38	2.04	1.42	3.89	4.62
	HL_ace	1.16	0.47	3.64	1.05	1.27	2.29	1.20	1.29	3.64	4.04
	HL_acf	1.16	0.48	3.75	0.74	1.95	0.83	1.16	2.11	3.75	4.46
	L_abc	0.50	−0.02	1.25	0.98	0.63	2.08	1.07	0.60	2.42	2.71
	L_abd	0.50	−0.04	1.35	0.98	1.22	1.67	1.07	1.18	2.26	2.77
	L_acb	0.55	−0.33	1.25	0.79	1.37	2.08	0.78	1.15	2.42	2.79
	L_acd	0.55	−1.03	2.96	0.79	1.37	1.53	0.78	1.67	2.96	3.49
Large lecture room	HH_abe	−0.02	−4.64	13.53	1.14	5.13	2.70	1.09	5.96	13.53	14.83
	HH_abf	−0.18	1.20	4.60	0.98	0.80	1.25	0.87	1.35	4.60	4.87
	HH_ace	0.07	0.23	5.44	2.20	3.48	2.90	1.71	3.21	5.44	6.54
	HH_acf	0.31	1.82	2.82	2.00	1.66	1.86	1.76	1.84	2.82	3.80
	HL_abe	−0.20	−5.06	12.85	1.37	5.18	2.73	1.26	6.38	12.85	14.40
	HL_abf	0.41	−0.06	7.09	1.20	1.94	2.01	1.11	1.79	7.09	7.39
	HL_ace	−0.28	−0.19	5.19	2.22	3.46	3.02	1.79	3.08	5.19	6.30
	HL_acf	0.64	−0.79	6.91	1.53	3.20	1.14	1.50	3.10	6.91	7.72
	L_abc	−0.78	0.64	4.21	1.05	0.92	1.80	1.09	1.02	4.21	4.46
	L_abd	−0.37	0.69	4.11	0.91	0.87	1.75	0.85	0.97	4.11	4.31
	L_acb	0.20	−0.28	4.21	1.03	0.85	1.80	0.93	0.80	4.21	4.38
	L_acd	0.46	−0.32	4.25	0.84	0.63	1.73	0.70	0.61	4.25	4.35

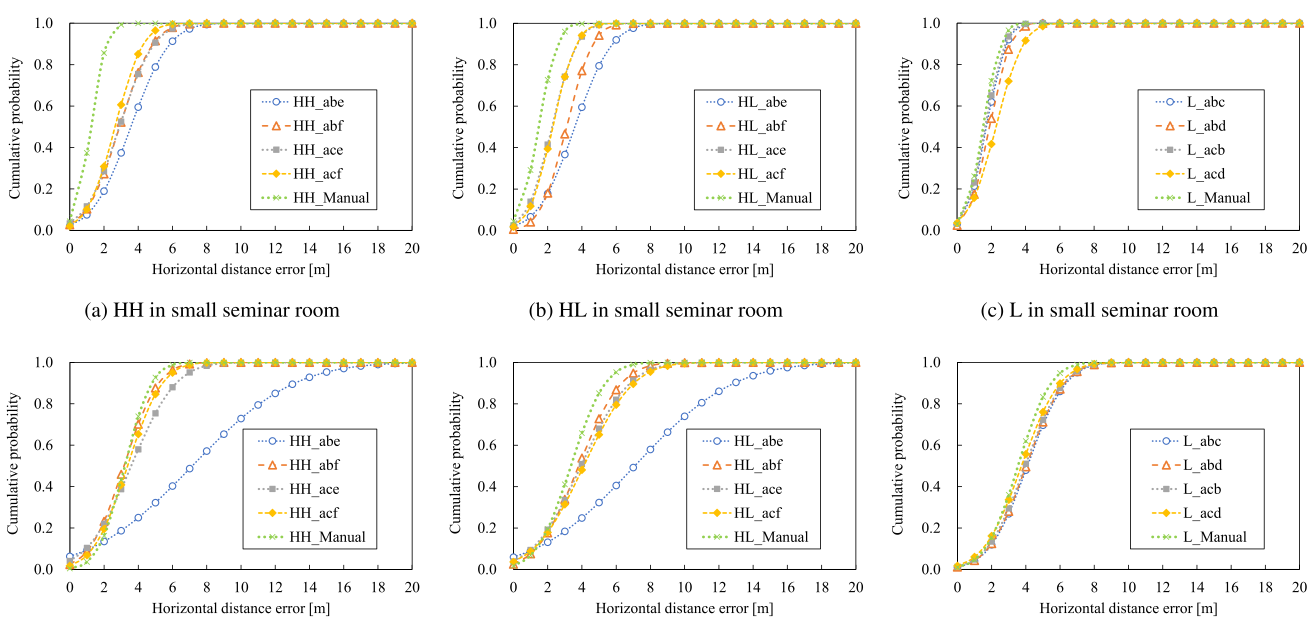

(a) HH in small seminar room (b) HL in small seminar room (c) L in small seminar room

(d) HH in large lecture room (e) HL in large lecture room (f) L in large lecture room

Fig. 6 Results of estimating the smartphone position.

than that in the large lecture room, but the height at which the AP was installed and the order in which the APs were activated had an influence on the positioning results.

In Table 4, the acquisition rates of the positioning results in the small seminar room were low (30~70%), but those in the large lecture room were at least 70%, regardless of the evaluation pattern. Given the true value of the AP installation location (i.e., the value denoted "Manual"), the acquisition rate is approximately 80% in the large lecture room, whereas it is approximately 50% in the small seminar room, suggesting that the rate depends on the environment (e.g., multipath). One of the reasons for the lower acquisition rates of the positioning result may be that the mean distance error between the AP and the smartphone became smaller, which prevented the intersection in the lateration, which did not allow the solution to converge in Eq. (7). In addition, there was no significant difference in smartphone position estimation performance by AP installation height.

Table 4 Results of estimating the smartphone position.

		Mean error of hor. dist. [m]	Positioning result acquisition rate [%]
Small seminar room	HH_abe	3.57	55.8
	HH_abf	2.92	32.4
	HH_ace	2.90	56.2
	HH_acf	2.65	37.3
	HH_Manual	1.23	50.4
	HL_abe	3.59	43.8
	HL_abf	3.10	48.6
	HL_ace	2.25	43.8
	HL_acf	2.29	64.0
	HL_Manual	1.48	51.4
	L_abc	1.72	68.6
	L_abd	1.90	68.6
	L_acb	1.65	68.8
	L_acd	2.27	68.8
	L_Manual	1.52	50.1
Large lecture room	HH_abe	7.15	84.4
	HH_abf	3.16	88.6
	HH_ace	3.59	84.5
	HH_acf	3.37	71.1
	HH_Manual	3.21	82.9
	HL_abe	7.09	84.0
	HL_abf	3.81	91.0
	HL_ace	3.95	84.1
	HL_acf	4.11	83.0
	HL_Manual	3.36	85.4
	L_abc	4.09	87.0
	L_abd	4.02	86.7
	L_acb	3.96	87.0
	L_acd	3.75	86.8
	L_Manual	3.54	78.2

In this experiment, the order of AP activation, which affects the coordinate axis settings, was also changed, which may have had a significant impact.

Wi-Fi RTT ranging accuracy is affected by the following: (1) propagation environment, (2) accuracy of AP and STA timestamps, (3) radio wave interference with devices using the same frequency band (e.g., radar systems), and (4) channel bandwidth. (1) The propagation environment (especially, LoS or NLoS) affects ranging performance (e.g., [12], [18], [19], [24], [29], [30], [32]). We conducted a prior experiment to calibrate the ranging offset between APs and between APs and smartphones. However, the bias error of the ranging results cannot be completely reduced to zero because it is not possible to determine LoS and NLoS only by the information of the received radio waves. (2) The accuracy of the timestamp affects ranging performance (e.g., [27]). The ranging offset was removed by the calibration in a prior experiment, however the ranging error caused by the variance of the timestamp could not be completely eliminated. By the way, since the mean of ranging errors caused by timestamps is reduced to almost zero by the prior calibration, these influences can be reduced by using the results of multiple measurements. (3) The least crowded channels (38 and 46 ch) in the experimental environments were used in the experiments. These channels are in the W52 band (5.15–5.25 GHz) and have no interference from other radio-wave systems such as radar systems. In addition, there were no Wi-Fi communication devices in and around the experimental environments during the experiment. (4) The actual ranging accuracy depends on the channel bandwidth (e.g., [12], [19], [20], [31], [32]). In addition, the official document from Android gives a statement [38] about the ranging accuracy in different channel bandwidths as: *"a range estimate is expected to have the following tolerances: 80 MHz: 2 meters, 40 MHz: 4 meters, 20 MHz: 8 meters."* If we can use the APs supporting the 80-MHz bandwidth, the positioning performance will be improved.

The primary application of the proposed method is indoor pedestrian LBS (e.g., navigation) using smartphones. Compared to the performance in "Manual," which was given manually by precisely measuring the AP installation location, the performance degradation was at most 1.69 m, except for "HH(HL)_abe." The performance deterioration at most 1.69 m is approximately two steps in terms of an adult's stride length. Considering pedestrian navigation in an indoor environment, even if the positioning result deviates by approximately two steps, there is little hindrance to movement. In other words, the Wi-Fi RTT lateration delivered high smartphone positioning performance without a pre-constructed database or precise AP location measurement. Nonetheless, it would be necessary to consider the combination of room sizes, heights at which APs are installed, and order in which APs are activated.

5. Conclusion

This paper proposed an algorithm for estimating the location of APs and evaluated the performance of this algorithm through experiments in real indoor environments. The proposed method enabled Wi-Fi RTT lateration to be realized without pre-constructing a database and without requiring precise measurements of AP installation locations. The proposed algorithm constructs a local coordinate system with the first four APs that are activated in turn, and estimates the AP installation location using Wi-Fi RTT lateration and the ranging results between APs. To confirm the effectiveness of the proposed algorithm, experiments were conducted to evaluate the positioning performance in real indoor environments. The experimental environment consisted of two rooms of different sizes. Wi-Fi RTT lateration delivered outstanding smartphone positioning performance without a pre-constructed database or precise AP location measurements.

Future plans include developing APs that fully support inter-AP ranging and the LCI report, and establishing an automatic method to correct inter-AP ranging errors. The aim is to use the proposed algorithm to estimate the flight position of unmanned aerial vehicles in fields with steep slopes and other complex terrains, where accurate and precise positioning is difficult.

Acknowledgments

This work is partly based on results obtained from a project, JPNP20004, subsidized by the New Energy and Industrial

Technology Development Organization (NEDO). The authors would like to thank Editage (www.editage.jp) for the English language review.

References

[1] M. Shiotsu, S. Yoshizawa, K. Ikeda, and A. Nozaki, "Survey on human activity patterns according to time and place: Basic research on the exposure dose to indoor air pollutants part 1," J. Archit. Plann. (Trans. AIJ), vol.63, no.511, pp.45–52, Sept. 1998 (in Japanese). DOI: 10.3130/aija.63.45_4
[2] J. Krumm and K. Hinckley, "The NearMe wireless proximity server," Proc. UbiComp 2004, Nottingham, UK, pp.283–300, Sept. 2004. DOI: 10.1007/978-3-540-30119-6_17
[3] J. Yin, Q. Yang, and L. Ni, "Adaptive temporal radio maps for indoor location estimation," Proc. PerCom 2005, Kauai, HI, USA, pp.85–94, March 2005. DOI: 10.1109/PERCOM.2005.7
[4] S. Ito and N. Kawaguchi, "Bayesian based location estimation system using wireless LAN," Proc. PerCom Workshops 2005, Kauai, HI, USA, pp.273–278, March 2005. DOI: 10.1109/PERCOMW.2005.19
[5] P. Bahl and V.N. Padmanabhan, "RADAR: An in-building RF-based user location and tracking system," Proc. INFOCOM 2000, Tel Aviv, Israel, pp.775–784, March 2000. DOI: 10.1109/INFCOM.2000.832252
[6] T. Manabe and T. Hasegawa, "A design methodology for positioning sub-platform on smartphone based LBS," IEICE Trans. Fundamentals, vol.E99-A, no.1, pp.297–309, Jan. 2016. DOI: 10.1587/transfun.E99.A.297
[7] B. Li, J. Salter, A.G. Dempster, and C. Rizos, "Indoor Positioning Techniques Based on Wireless LAN," Proc. ICUWB 2006, Sydney, Australia, pp.13–16, Jan. 2006.
[8] X. Li, K. Pahlavan, M. Latva-aho, and M. Ylianttila, "Comparison of indoor geolocation methods in DSSS and OFDM wireless LAN systems," Proc. VTC Fall 2000, Boston, MA, USA, pp.3015–3020, Sept. 2000. DOI: 10.1109/VETECF.2000.886867
[9] A. Günther and C. Hoene, "Measuring round trip times to determine the distance between WLAN nodes," Proc. Networking 2005, Waterloo, Canada, pp.768–779, May 2005. DOI: 10.1007/11422778_62
[10] M. Ciurana, F. Barcelo-Arroyo, and F. Izquierdo, "A ranging system with IEEE 802.11 data frames," Proc. RWW 2007, Long Beach, CA, USA, pp.133–136, Jan. 2007. DOI: 10.1109/RWS.2007.351785
[11] IEEE Standards Association, IEEE Std 802.11-2016, IEEE Standard for Information Technology — Telecommunications and information exchange between systems Local and metropolitan area networks — Specific requirements, Part 11: Wireless LAN Medium Access Control (MAC) and Physical Layer (PHY) Specifications, Dec. 2016. DOI: 10.1109/IEEESTD.2016.7786995
[12] T. Manabe, K. Aihara, N. Kojima, Y. Hirayama, and T. Suzuki, "A design methodology of Wi-Fi RTT ranging for lateration," IEICE Trans. Fundamentals, vol.E104-A, no.12, pp.1704–1713, Dec. 2021. DOI: 10.1587/transfun.2020EAP1129
[13] M. Ibrahim, H. Liu, M. Jawahar, V. Nguyen, M. Gruteser, R. Howard, B. Yu, and F. Bai, "Verification: Accuracy evaluation of WiFi fine time measurements on an open platform," Proc. MobiCom 2018, New Delhi, India, pp.417–427, Oct. 2018. DOI: 10.1145/3241539.3241555
[14] N. Jathe, M. Lütjen, and M. Freitag, "Indoor positioning in car parks by using Wi-Fi round-trip-time to support finished vehicle logistics on port terminals," IFAC-PapersOnLine, vol.52, no.13, pp.857–862, Dec. 2019. DOI: 10.1016/j.ifacol.2019.11.237
[15] Y.B. Bai, A. Kealy, G. Retscher, and L. Hoden, "A comparative evaluation of Wi-Fi RTT and GPS based positioning," Proc. IGNSS Symp. 2020, Sydney, Australia, pp.1–12, Feb. 2020.
[16] M. Ogawa and H. Choi, "Measurement accuracy of Wi-Fi FTM on actual devices," IEICE Commun. Express, vol.9, no.12, pp.567–572, Dec. 2020. DOI: 10.1587/comex.2020COL0001
[17] W. Unuma, T. Manabe, and K. Aihara, "Access point selection method on Wi-Fi RTT-based positioning," IEICE Technical Report, ITS2021-4, July 2021 (in Japanese).
[18] M. Si, Y. Wang, S. Xu, M. Sun, and H. Cao, "A Wi-Fi FTM-based indoor positioning method with LOS/NLOS identification," Appl. Sci., vol.10, no.3, p.956, Feb. 2020. DOI: 10.3390/app10030956
[19] Y. Yu, R. Chen, Z. Liu, G. Guo, F. Ye, and L. Chen, "Wi-Fi fine time measurement: Data analysis and processing for indoor localisation," J. Navig., vol.73, no.5, pp.1106–1128, Sept. 2020. DOI: 10.1017/S0373463320000193
[20] C. Ma, B. Wu, S. Poslad, and D.R. Selviah, "Wi-Fi RTT ranging performance characterization and positioning system design," IEEE Trans. Mobile Comput., vol.21, no.2, pp.740–756, July 2020. DOI: 10.1109/TMC.2020.3012563
[21] N. Dvorecki, O. Bar-Shalom, L. Banin, and Y. Amizur, "A machine learning approach for Wi-Fi RTT ranging," Proc. ION ITM 2019, Reston, VA, USA, pp.435–444, Jan. 2019. DOI: 10.33012/2019.16702
[22] J. Choi, Y.-S. Choi, and S. Talwar, "Unsupervised learning techniques for trilateration: From theory to android APP implementation," IEEE Access, vol.7, pp.134525–134538, Sept. 2019. DOI: 10.1109/ACCESS.2019.2941657
[23] S. Yan, H. Luo, F. Zhao, W. Shao, Z. Li, and A. Crivello, "Wi-Fi RTT based indoor positioning with dynamic weighted multidimensional scaling," Proc. IPIN 2019, pp.1–8, Sept./Oct. 2019. DOI: 10.1109/IPIN.2019.8911783
[24] J.-H. Seong, S.-H. Lee, W.-Y. Kim, and D.-H. Seo, "High-precision RTT-based indoor positioning system using RCDN and RPN," Sensors, vol.21, no.11, May 2021. DOI: 10.3390/s21113701
[25] L. Banin, U. Schatzberg, and Y. Amizur, "WiFi FTM and map information fusion for accurate positioning," Proc. IPIN 2016, Madrid, Spain, pp.1–4, Oct. 2016.
[26] J.T. Biehl, A. Girgensohn, and M. Patel, "Achieving accurate room-level indoor location estimation with emerging IoT networks," Proc. IoT 2019, Bilbao, Spain, pp.1–8, Oct. 2019. DOI: 10.1145/3365871.3365875
[27] G. Guo, R. Chen, F. Ye, X. Peng, Z. Liu, and Y. Pan, "Indoor smartphone localization: A hybrid WiFi RTT-RSS ranging approach," IEEE Access, vol.7, pp.176767–176781, Dec. 2019. DOI: 10.1109/ACCESS.2019.2957753
[28] S. Xu, R. Chen, Y. Yu, G. Guo, and L. Huang, "Locating smartphones indoors using built-in sensors and Wi-Fi ranging with an enhanced particle filter," IEEE Access, vol.7, pp.95140–95153, July 2019. DOI: 10.1109/ACCESS.2019.2927387
[29] M. Sun, Y. Wang, S. Xu, H. Qi, and X. Hu, "Indoor positioning tightly coupled Wi-Fi FTM ranging and PDR based on the extended Kalman filter for smartphones," IEEE Access, vol.8, pp.49671–49684, March 2020. DOI: 10.1109/ACCESS.2020.2979186
[30] Y. Yu, R. Chen, L. Chen, S. Xu, W. Li, Y. Wu, and H. Zhou, "Precise 3-D indoor localization based on Wi-Fi FTM and built-in sensors," IEEE Internet Things J., vol.7, no.12, pp.11753–11765, June 2020. DOI: 10.1109/JIOT.2020.2999626
[31] J. Choi and Y.-S. Choi, "Calibration-free positioning technique using Wi-Fi ranging and built-in sensors of mobile devices," IEEE Internet Things J., vol.8, no.1, pp.541–554, Jan. 2021. DOI: 10.1109/JIOT.2020.3004774
[32] K. Han, S.M. Yu, S.-L. Kim, and S.-W. Ko, "Exploiting user mobility for WiFi RTT positioning: A geometric approach," IEEE Internet Things J., vol.8, no.19, pp.14589–14606, Oct. 2021. DOI: 10.1109/JIOT.2021.3070367
[33] J.A. López-Pastor, P. Arques-Lara, J.J. Franco-Peñaranda, A.J. García-Sánchez, and J.L. Gómez-Tornero, "Wi-Fi RTT-based active monopulse RADAR for single access point localization," IEEE Access, vol.9, pp.34755–34766, Feb. 2021. DOI: 10.1109/ACCESS.2021.3062085
[34] C.S. Álvarez-Merino, H.Q. Luo-Chen, E.J. Khatib, and R. Barco, "WiFi FTM, UWB and cellular-based radio fusion for indoor positioning," Sensors, vol.21, no.21, Oct. 2021. DOI: 10.3390/

s21217020
[35] J. Choi, Y.-S. Choi, and S. Talwar, "Unsupervised learning technique to obtain the coordinates of Wi-Fi access points," Proc. IPIN 2019, Pisa, Italy, Sept. 2019. DOI: 10.1109/IPIN.2019.8911824
[36] M. Fujii, "A study on high accuracy positioning by extended FTM network," IEICE Technical Report, ITS2020-18, Dec. 2020 (in Japanese).
[37] Y. Hirayama, N. Kojima, T. Suzuki, and T. Manabe, "Performance evaluation of indoor positioning method using Wi-Fi RTT," IEICE Technical Report, ITS2019-61, March 2020 (in Japanese).
[38] Android Open Souce Project, "Wi-Fi RTT (IEEE 802.11mc)," https://source.android.com/devices/tech/connect/wifi-rtt, accessed Aug. 29, 2022.

Tetsuya Manabe received his B.E., M.E., and Ph.D. degrees in Electrical and Electronic Systems from Saitama University, in 2006, 2008, and 2012, respectively. He is an Assistant Professor in the Division of Mathematics, Electronics and Informatics, Graduate School of Science and Engineering, Saitama University. His research interest include ICT-based systems innovation for human mobility sophistication, with a specific focus on realizing information society infrastructure, e.g., pedestrian navigation systems with seamless positioning and navigation/riding safety support systems for slow vehicles (including bicycles). He is a member of the Institute of Electronics, Information and Communication Engineers (IEICE), the Institute of Electrical and Electronics Engineers (IEEE), the Information Processing Society of Japan (IPSJ), the Japan Society of Civil Engineers (JSCE), and the Japan Society of Traffic Engineers (JSTE).

Kazuya Saba received his B.E. degree in Electrical and Electronic Systems from Saitama University in 2022. He has studied the positioning environment construction using Wi-Fi RTT.